

Magnetic behavior of nanocrystals of the spin-chain system $\text{Ca}_3\text{Co}_2\text{O}_6$: Absence of multiple steps in the low-temperature isothermal magnetization

Niharika Mohapatra, Kartik K. Iyer, Sitikantha D. Das, B. A. Chalke, S. C. Purandare, and E. V. Sampathkumaran*

Tata Institute of Fundamental Research, Homi Bhabha Road, Colaba, Mumbai 400005, India

(Received 1 January 2009; revised manuscript received 30 March 2009; published 27 April 2009)

We report that the major features in the temperature dependence of dc and ac magnetizations of a well-known spin-chain compound $\text{Ca}_3\text{Co}_2\text{O}_6$, which has been known to exhibit two complex magnetic transitions due to geometrical frustration (one near 24 K and the other near 10 K), are found to be qualitatively unaffected in its nanomaterials synthesized by high-energy ball milling. However, the multiple steps in isothermal magnetization—a topic of current interest in low-dimensional systems—known for the bulk form well below 10 K is absent in the nanoparticles. We believe that this finding will be useful to the understanding of the “step” magnetization behavior of such spin-chain systems.

DOI: [10.1103/PhysRevB.79.140409](https://doi.org/10.1103/PhysRevB.79.140409)

PACS number(s): 75.60.Ej, 75.40.Cx, 75.50.Lk

The existence of the plateaus in the isothermal magnetization (M) of spin-chain systems has been attracting considerable attention of condensed-matter theorists as well as experimentalists.¹ In this respect, the spin-chain compound $\text{Ca}_3\text{Co}_2\text{O}_6$, crystallizing in the K_4CdCl_6 -type rhombohedral structure, is of great interest in the current literature, as there is one step in M in an intermediate temperature (T) range (~ 10 – 24 K) at one third of saturation magnetization (M_s), but there are multiple steps at much lower temperatures at an equal spacing of 12 kOe.^{2–4} It is now well known that the ferromagnetic spin chains are arranged in a triangular fashion in the basal plane with an interchain antiferromagnetic interaction leading to geometrical frustration in this compound; as a result, two out of three chains order antiferromagnetically and the third one remains incoherent (in the range 10–24 K) or undergoes a complex ordering (below 10 K). With this scenario, the plateau at $M_s/3$ for the range 10–24 K is understandable in terms of a field-induced ferrimagnetic alignment,² but it is difficult to explain the step behavior at lower temperatures. Various explanations have been proposed^{4–10} in the literature for the origin of multistep behavior below 10 K, for example, (i) magnetic field (H)-induced transitions between different spin states,^{4,7} and (ii) quantum tunneling effects similar to that known for molecular magnets and a complex relaxation process.^{5,6}

Apart from the above magnetization behavior, this compound provides a unique opportunity to understand geometrically frustrated magnetism of spin chains. The magnetic state in the range 10–24 K is called “partially disordered antiferromagnetism (PDA).” Interesting anomalies have been found in many spectroscopic and bulk studies, including magneto-dielectric coupling and thermopower from the applications point of view.^{11–21} While all these studies have been carried out on bulk single crystals or polycrystals, there is not much work on the nanocrystalline form. There were two reports²² on the isothermal M behavior at 10 K on the films grown on different substrates by pulsed laser ablation method and the results appear to differ. In addition, it is not clear how these “steps” in $M(H)$ behave at further low temperatures in these films. In order to advance the understanding of the properties of this compound in general, it is important to clarify whether the magnetic properties are preserved down to nanoscale, particularly, noting that the magnetic correlation length

scale along c axis has been experimentally determined to be on the order of 550 nm along c axis, whereas it is on the order of 18 nm along basal plane.^{14,15} We have therefore synthesized the fine particles in nanometer range by high-energy ball-milling method²³ and studied its magnetization behavior; the results of which are reported here.

The polycrystalline samples in the bulk form (called “ B ”) have been prepared by a conventional solid-state reaction route¹¹ and characterized by x-ray diffraction (XRD) ($\text{Cu } K_\alpha$) to be single phase (within the detection limit of 2%). The compound, after characterizing by magnetic studies as well, were milled for 8 h in a planetary ball mill (Fritsch pulverisette-7 premium line) operating at a speed of 500 rpm in a medium of toluene to attain nanosized (called “ N ”) particles. Tungsten carbide vials and balls of 5 mm diameter were used with a balls-to-material mass ratio of 10:1. To characterize the specimens, apart from x-ray diffraction, scanning electron microscope (SEM) and transmission electron microscope [(TEM) Tecnai 200 kV] were employed. The dc $M(T)$ measurements (in the range 1.8–300 K) were performed employing a commercial superconducting quantum interference device [(SQUID) Quantum Design] and the same magnetometer was employed to take ac susceptibility (χ_{ac}) data. $M(H)$ (up to 120 kOe) measurements at selected temperatures were carried out employing a commercial vibrating sample magnetometer [(VSM) Oxford Instruments].

Figure 1(a) shows the XRD pattern for the milled specimen. All reflections expected are present in the milled specimen and there is no change in the shape of the background with respect to that of the bulk. There is negligible change in the lattice constants [for B : $a=9.076(2)$ Å, $c=10.379(2)$ Å; for N , $a=9.069(2)$ Å, $c=10.393(2)$ Å] obtained by Rietveld fitting. The pattern for the milled sample is more broadened attributable to a decrease in particle size, as shown in the inset of Fig. 1(a). An idea of the average particle size (about 50 nm) could be inferred from the width of the most intense line (after subtracting instrumental line broadening) employing Debye-Scherrer formula. Attempts to eliminate corrections for strain effects employing Williamson-Hall plots were not successful, as such plots are not found to be linear, possibly due to a large spread in the particle sizes. In order to get a better idea about the particle size, we have employed SEM and TEM. According to the

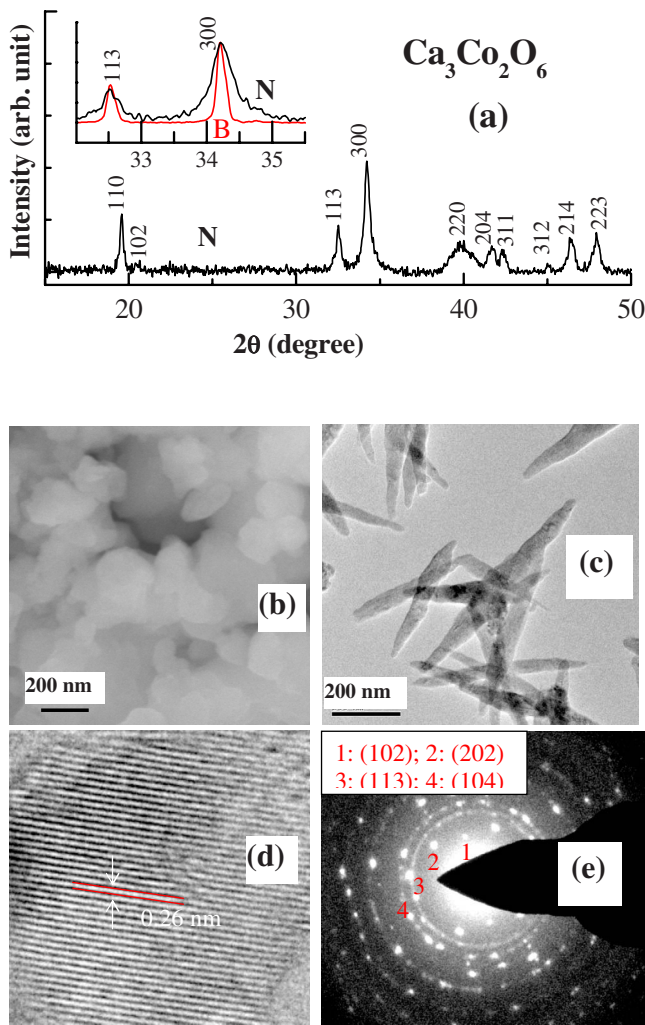


FIG. 1. (Color online) (a) X-ray diffraction pattern (Cu K_{α}), (b) SEM images, (c) TEM images of nanorods, (d) high-resolution TEM showing (300) lattice planes, and (e) selected area diffraction pattern obtained by TEM with indexing of four innermost diffraction rings, for the ball-milled specimens of $\text{Ca}_3\text{Co}_2\text{O}_6$. In (a), the x-ray diffraction pattern for two lines are compared for the bulk and nanoparticles to show line broadening (after normalizing to respective peak heights).

SEM images shown in Fig. 1(b), the particles attained nanometer dimensions (typically below 100 nm) with significant agglomeration. We have isolated some of the particles by ultrasonification in alcohol and obtained the bright-field TEM images. These images shown in Fig. 1(c) reveal that these particles are rod shaped with a typical length of a few hundred nanometers and a width of less than 50 nm. It is interesting to note that the ball-milling conditions employed yields nanorods, which otherwise could be obtained by laser ablation only on Si(100) substrate. High-resolution TEM images [see Fig. 1(d), for instance, for (300) plane] reveal well-defined lattice planes, thereby confirming that the nanospecimens are crystalline and not amorphous. We have also obtained the selected area electron-diffraction pattern [see Fig. 1(e)] and all the diffraction rings are indexable to the compound under investigation, thereby confirming that the nanospecimens corresponds to the parent compound and

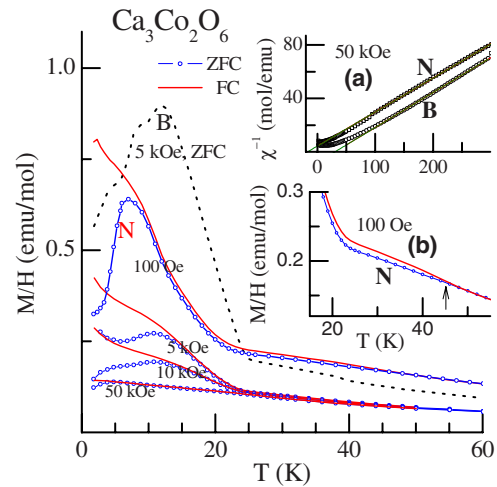


FIG. 2. (Color online) Magnetization (M) divided by magnetic field (H), measured in the presence of several fields below 60 K for the nanoparticles (N) of $\text{Ca}_3\text{Co}_2\text{O}_6$. The ZFC curve obtained in 5 kOe for the bulk specimen (B) is also shown for comparison. In inset (a), inverse susceptibility obtained in a field of 50 kOe is plotted for both the specimens and the straight lines in these cases are obtained by Curie-Weiss fitting of the data above 100 K. In inset (b), the magnetic-susceptibility curves obtained in a field of 100 Oe for the zero-field-cooled and field-cooled conditions of the nanospecimen are shown in an expanded form to highlight apparent bifurcation around 45 K. The lines through the data points serve as guides for the eyes.

these are polycrystalline; the appearance of some bright spots along the diffraction rings reveals that the particles are highly textured. Polycrystalline nature of the rods was also confirmed by dark field images (not shown here).

The results of dc and ac magnetization as a function of temperature measured in the presence of various magnetic fields ($H=100$ Oe, 5 kOe, 10 kOe, and 50 kOe) are shown in Figs. 2 and 3. For comparison, a curve obtained in a field of 5 kOe for the zero-field-cooled (ZFC) condition (ZFC, from

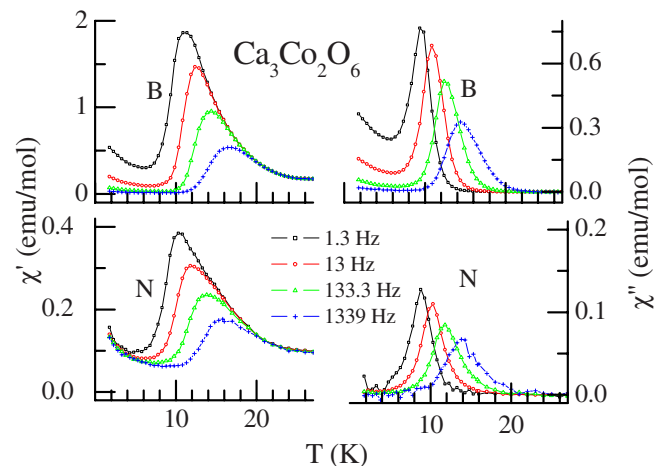


FIG. 3. (Color online) Real (χ') and imaginary (χ'') parts of ac susceptibility measured at various frequencies (with a ac field of 1 Oe) for bulk and nanoparticles of $\text{Ca}_3\text{Co}_2\text{O}_6$. The lines through the data points serve as guides for the eyes.

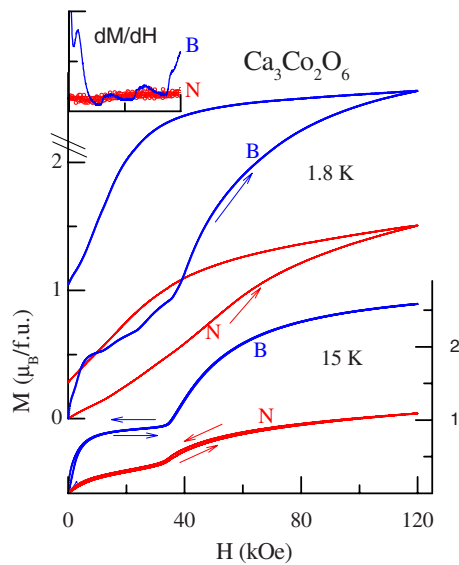


FIG. 4. (Color online) Isothermal M at 1.8 and 15 K for the bulk and nanoparticles of $\text{Ca}_3\text{Co}_2\text{O}_6$ for a sweep rate of H of 4 kOe/min. In the inset, the derivative of M below 40 kOe is plotted for both specimens.

100 K) for the bulk form^{3,4,11} is also shown. From the mainframe of Fig. 2, it is obvious that there is a sudden upturn in magnetization measured in low fields ($\ll 50$ kOe) near ($T_1=$) 24 K, with a peak in the ZFC curve at a lower temperature ($T_2 \sim 8$ –10 K). Application of high fields (say, 50 kOe) broadens the features at these transitions. These features, similar to those observed for the bulk form, imply that T_1 and T_2 are essentially unaffected by reducing the particle size. As a characteristic feature of PDA ordering between T_1 and T_2 , the dc χ curves are strongly field dependent similar to that known for **B**. In order to address whether there is any change in the magnetic moment on Co, we have performed dc χ measurements up to 300 K in the presence of a field of 50 kOe. As shown in the inset of Fig. 2, the plot of inverse χ versus T is linear over a wide T range (100–300 K), and the effective moment obtained from the linear region is about $5.6 \pm 0.05 \mu_B$ per formula unit, which is essentially the same as that of bulk. This implies that the electronic configuration of Co remains unaffected as one goes from bulk to nanoform. However, the sign of paramagnetic Curie temperature (~ -20 K) for **N** is negative, whereas it is positive for **B** (~ 35 K), as though the net dominating correlation is antiferromagnetic for **N**, precise reason of which is not clear to us at the moment. Otherwise, the above results reveal that the gross magnetic features of **B** are retained in **N**.

The χ_{ac} curves for **N** also look similar (Fig. 3) to that of **B** in the sense that there is a peak in both real (χ') and imaginary (χ'') parts, exhibiting a huge frequency (ν) dependence, with the χ' -peak temperature moving from 10 K for 1 Hz to 16 K for 1.339 kHz, implying that the spin dynamics are undisturbed when the particle size is reduced in this temperature range. We had earlier reported²⁰ that Arrhenius relation is obeyed; we estimate the activation energy from this relationship to be about 145 K, which is in good agreement with Hardy *et al.*⁶ An upward curvature in the real part of χ_{ac} reported by Hardy *et al.*⁶ in single crystals at very low tem-

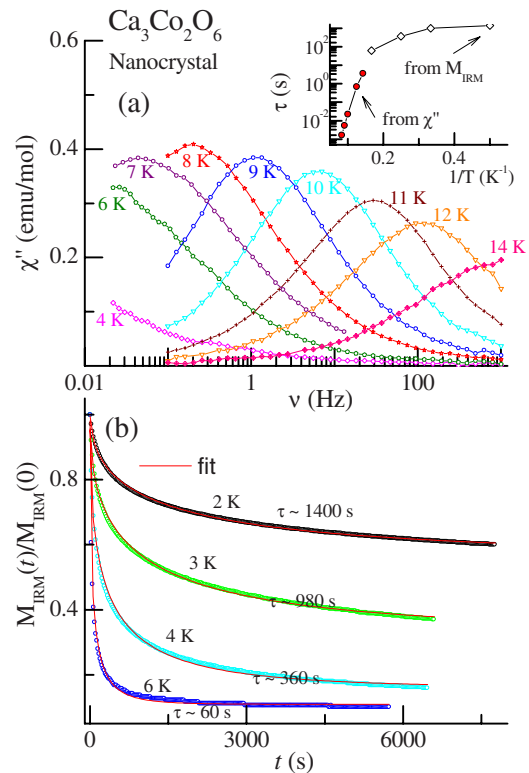


FIG. 5. (Color online) (a) χ'' as a function of frequency (ν) ($H_{ac}=3$ Oe) for the nanocrystals of $\text{Ca}_3\text{Co}_2\text{O}_6$. The inset shows the relaxation-time behavior. The lines through the data points serve as guides for the eyes. (b) Normalized isothermal remnant magnetization curves as a function of time.

peratures (< 5 K) and attributed to an intriguing change in spin dynamics could be observed in the specimen **N** as well.

We now look at the $M(H)$ behavior (see Fig. 4), which were taken for the ZFC condition of the specimens. We have chosen one temperature well below T_2 and another between T_1 and T_2 , viz., 1.8 and 15 K, to drive the messages. We note that for **N**, the magnetic moment does not get saturated even at fields as high as 120 kOe and the value of the magnetic moment at 120 kOe is significantly lower (nearly half) than that of the specimen **B**. Also, the $M(H)$ curve (at 1.8 K) is hysteretic. These features may support the inference from the paramagnetic Curie temperature that antiferromagnetic correlation tend to dominate when the particle dimension is reduced. With respect to steps in $M(H)$ —as mentioned earlier—for the specimen **B**, for $T=15$ K, there is a plateau at nearly $M_s/3$ and this feature appears manifesting itself as a distinct upturn in M near 35 kOe for **N**, pointing to the fact that PDA order is maintained at this temperature in the nanoform as well. For $T=1.8$ K, the multiple steps clearly appearing in single crystals⁴ are usually weakened in polycrystalline bulk samples and appear as a change in the slope of $M(H)$ plot. The derivative of M with respect H reveals minima at these steps in $M(H)$, as shown in the inset of Fig. 4. These steps are irreversible at this temperature. It is clear from Fig. 4 that the features are absent for the specimen **N** and dM/dH undergoes negligible variation (until the field of interest of 60 kOe) without exhibiting any minimum. This is interesting, particularly, noting that the behavior above T_2 for

N is essentially unaffected with respect to that for B .

As mentioned earlier, different concepts have been proposed for the multistep $M(H)$ behavior and characteristic ac and dc magnetization behavior and magnetic relaxation curves have been established for the single crystals in the past.^{4,5} In order to explore whether these characteristic features are still retained for N , we took additional magnetic data for N . We have obtained the $M(H)$ curves with VSM for different rates of change of H (100 Oe/min to 10 kOe/min) and it was found that the behavior is independent of the rate of change in field. In fact, the curves for varying sweep rates of field are found to lie one over the other. This situation is different from that reported for the bulk single crystals,⁵ in which case, the steps get more prominent with an increasing rate of change of H . In order to understand the behavior of spin-relaxation time (τ), we have measured with SQUID the imaginary part (χ'') of χ_{ac} as a function of ν (0.03 Hz–1 kHz) at several temperatures below 14 K after cooling the sample in zero field to the desired temperature and obtained $\tau(=1/2\pi\nu_m)$ from the knowledge of ν_m at which χ'' exhibits a peak. It is straightforward to conclude from the comparison of the curves in Fig. 5(a) with those reported for the single crystals by Hardy *et al.* in Fig. 2b in Ref. 6 that the τ values fall to comparatively much higher values with decreasing temperature for N ; for instance, a distinct peak in χ'' could be seen near 0.3 Hz for $T=2.25$ K in single crystals; whereas for N , no peak could be observed above 0.03 Hz even at 4 K. Since we cannot measure χ'' in the ν range below 0.03 Hz with our magnetometer, we have inferred the trend in τ for $T \leq 6$ K by isothermal remnant magnetization (M_{IRM}) behavior (measured with VSM). For this purpose, following the procedure adopted for single crystals by Maignan *et al.*,⁶ after the application of a magnetic field of a high field (say, 70 kOe), M_{IRM} in zero field was tracked as a function of time (t). M_{IRM} decays with t [see Fig. 5(b)] and, by fitting the curve to a stretched exponential of the form, $M_{IRM}=a+b \exp[-(t/\tau)^{0.5}]$ (where a and b are constants), we have estimated the values of τ . Qualitatively speaking, a combined look at the values of τ determined from both methods [see inset of Fig. 5(a)] reveals that τ exhibits thermally activated behavior well above 6 K with values less than few seconds and there is a crossover regime near T_2 at which τ

increases to several minutes increasing monotonically with T ; for instance, from ~ 60 s at 6 K to ~ 1400 s at 2 K. It is therefore concluded that the constancy of the value seen for the single crystal below 6 K is absent for N . These findings suggest that the concepts of quantum tunneling and multiple-spin states proposed for bulk form need not be considered for N . This observation raises a question whether the multiple-step $M(H)$ feature for the bulk form is characterized by a length scale much larger than the dimensions of the nanoparticle, particularly, noting that the magnetic correlations lengths (see the earlier part of this Rapid Communication) are of comparable magnitudes as those of N . Alternatively, a possible difference in the magnetic structure (below 10 K) between B and N could also be responsible for the modification of the low-temperature magnetization behavior.

We have made another interesting finding in the dc χ plot. It is known^{3,4} that ZFC and FC curves tend to bifurcate near T_2 in the bulk form. A careful look at the data for N measured with low fields, say for $H=100$ Oe, revealed (see inset b of Fig. 2) that the bifurcation sets in at a much higher temperature, well above T_1 (near 45 K), similar to the behavior noted for nanorods and thin films.²² This finding seems to endorse our previous claim^{17,21} with respect to additional interesting physics in the higher-temperature range.

Summarizing, the central point of emphasis is that the nanoparticles of the geometrically frustrated spin-chain compound $\text{Ca}_3\text{Co}_2\text{O}_6$ synthesized by high-energy ball milling do not show multiple-step isothermal magnetization behavior noted for the bulk form of this compound at low temperatures. However, other qualitative features in the magnetic susceptibility remain essentially unaltered compared to the bulk. We believe that this work would motivate an extension of such studies to the nanoparticles of other spin-chain systems to clarify pertinent issues. Another finding we made from the low-field magnetic-susceptibility data is that there exists another magnetic anomaly above 40 K. Finally, this work provides a route to make large quantities of nanoparticles of this spin-chain oxide and its derivatives in stable form to enable further studies and potential applications.

We thank N. R. Selvi Jawaharlal Nehru Center for Advanced Scientific Research, Bangalore, India, for SEM data.

*sampath@mailhost.tifr.res.in

¹See, for example, T. Vekua *et al.*, Phys. Rev. Lett. **96**, 117205 (2006).

²S. Aasland *et al.*, Solid State Commun. **101**, 187 (1997).

³H. Kageyama *et al.*, J. Phys. Soc. Jpn. **66**, 1607 (1997).

⁴A. Maignan *et al.*, Eur. Phys. J. B **15**, 657 (2000).

⁵V. Hardy *et al.*, Phys. Rev. B **70**, 064424 (2004).

⁶V. Hardy *et al.*, Phys. Rev. B **70**, 214439 (2004); A. Maignan *et al.*, J. Mater. Chem. **14**, 1231 (2004).

⁷H. Wu *et al.*, Phys. Rev. Lett. **95**, 186401 (2005).

⁸Yu. B. Kudasov *et al.*, Phys. Rev. B **78**, 132407 (2008).

⁹X. Yao *et al.*, Phys. Rev. B **74**, 134421 (2006).

¹⁰R. Sato *et al.*, arXiv:0811.4772 (unpublished).

¹¹S. Rayaprol *et al.*, Solid State Commun. **128**, 79 (2003); E. V. Sampathkumaran *et al.*, Phys. Rev. B **70**, 014437 (2004); E. V. Sampathkumaran *et al.*, J. Magn. Magn. Mater. **284**, L7 (2004).

¹²K. Takubo *et al.*, Phys. Rev. B **71**, 073406 (2005).

¹³T. Burnus *et al.*, Phys. Rev. B **74**, 245111 (2006).

¹⁴A. Bombardi *et al.*, Phys. Rev. B **78**, 100406(R) (2008); S. Agrestini *et al.*, *ibid.* **77**, 140403(R) (2008).

¹⁵S. Agrestini *et al.*, Phys. Rev. Lett. **101**, 097207 (2008).

¹⁶S. Takeshita *et al.*, J. Phys. Soc. Jpn. **75**, 034712 (2006); J. Sugiyama *et al.*, Phys. Rev. B **72**, 064418 (2005).

¹⁷P. L. Paulose *et al.*, Phys. Rev. B **77**, 172403 (2008).

¹⁸N. Bellido *et al.*, Phys. Rev. B **77**, 054430 (2008).

¹⁹M. Mikami *et al.*, J. Appl. Phys. **94**, 6579 (2003).

²⁰S. Rayaprol *et al.*, Proc.-Indian Acad. Sci., Chem. Sci. **115**, 553 (2003).

²¹R. Bindu *et al.*, Phys. Rev. B **79**, 094103 (2009).

²²P. L. Li *et al.*, Appl. Phys. Lett. **91**, 042505 (2007); R. Moubah *et al.*, *ibid.* **91**, 172517 (2007).

²³C. Suryanarayana, Prog. Mater. Sci. **46**, 1 (2001).